A STOCHASTIC ANALYSIS OF PRESSURE FLUCTUATION IN A FLUIDIZED BED REACTOR

by

DEBASHIS NEOGI

B.Tech. (Chem. Engg.), Indian Institute of Technology, 1981
M.S. (Chem. Engg.), Kansas State University, 1984

MASTER'S REPORT

submitted in partial fulfillment of the

requirements for the degree

MASTER OF SCIENCE

Department of Statistics

KANSAS STATE UNIVERSITY
Manhattan, Kansas

1987

Approved by:

R Nassar
Major Professor

ACKNOWLEDGEMENT

I wish to express my gratitude to Dr. R. Nassar and Dr. L . T. Fan for their invaluable guidance and helpful criticism throughout the course of this work. I sincerely thank Dr. K. E. Kemp for consenting to sit in my committee.

I wish to thank my parents, Mr. and Mrs. S. K. Neogi for their support and encouragement during my graduate work at Kansas State University. I would also like to thank my friends and colleagues for their continuous encouragement.

ALL MODELS ARE WRONG, BUT SOME OF THEM ARE USEFUL.

George Box

TABLE OF CONTENTS

LIST OF TABLES

LIST OF FIGURES

INTRODUCTION

Pressure fluctuations have been observed to occur in most fluidized beds and these fluctuations have been used to define an index for the quality of fluidization (Shuster and Kisliak, 1952; Sutherland, 1964; Winter, 1968). Small and rapid fluctuations are considered to be associated with a good quality of fluidization. It appears that analyzing the relationship between pressure fluctuations and bubble behavior in a gas-solid fluidized bed gives rise to effective information on control strategies for the system (Jones and Pyle, 1971; Whitehead et al., 1977). The nature of pressure fluctuations in a fluidized bed is a complex function of particle properties, bed geometry, pressure in the bed, and properties and flow conditions of the fluidizing fluid.

Pressure fluctuations have been studied by numerous investigators (Tamarin, 1964; Swinehart, 1966; Hiby, 1967; Kang et al., 1967; Lirag and Littman, 1971; Wong and Baird, 1971; Fan et al., 1981). They have drawn essentially two different conclusions about the cause of pressure fluctuations in a fluidized bed. Tamarin (1964) and Hiby (1967) have concluded that the pressure fluctuations are related to the passage of bubbles through the upper boundary of the bed and to the changes in the height of the bed. Similarly Lirag and Littman (1971) have revealed that the fluctuating signals of pressure involve the periodic

component resulting from the bubbles escaping from the surface of the fluidized bed. Kang et al. (1967), however, have concluded that the action of bubbles causes changes in the mode and condition of gas flow and porosity in the dense phase, inducing the pressure fluctuations. Hiby (1967) also has proposed a deterministic model, which recognizes the presence of periodic components; the frequency of the whole bed is estimated from the assumed frequencies of individual particles. Moritomi et al. (1980) have established a deterministic model taking into account inertia, damping and frictional forces.

Statistical methods were employed fairly extensively by previous investigators (see, e.g. Swinehart, 1966; Kang et al., 1967; Lirag and Littman, 1971; Fan et al, 1981) used statistical approaches. Swinehart (1966) calculated the cross-correlation function between two pressure fluctuation signals taken from two vertically separated pressure taps and determined the "correlation-average propagation velocity" of bubbles in a fluidized bed. Kang et al. (1967) and Lirag and Littman (1971) calculated the probability density, auto-correlation function, and power spectral density functions of the pressure fluctuations off-line. The resultant auto-correlation and power spectral density functions were then used to determine the frequency of the fluctuations. Lirag and Littman (1971) also used the measured frequency to estimate the bubble

size. These investigators have amply demonstrated the power of the statistical analysis or correlation approach in analyzing the random pressure fluctuation signals in a fluidized bed; nevertheless relatively little has been done to stochastically model the phenomena of pressure fluctuations.

Hiby (1967) has predicted theoretically that frequency should decrease with increased velocity but has failed to prove it experimentally. Jones and Pyle (1971) found that frequency increased with the superficial velocity, u, to the undamped natural frequency of the system; but, no effect of u was found for particles with a size of 500 μ. Lirag and Littman (1971) observed that the frequency increased slightly with the superficial velocity except in the shallow beds of 500 μ glass particles. The experimental or theoretical results of the various investigators appear to contradict each other either. This contradiction need be resolved, which is the objective of the present study.

In the work reported in this paper, pressure fluctuations due to the bubble movement near the distributor plate were measured by means of a pressure probe over a range of time. The resultant time-series have been analyzed off-line by determining their auto-correlation function and power spectrum with emphasis on the effect of the superficial velocity of the fluidizing

gas. A stochastic model of bubble motion in a fluidized bed has been developed. This model visualizes the bubble motion in a fluidized bed to consist of the random movement, generating irregular signals, and the linear movement, generating wave-like signals. A theoretical auto-correlation function and the corresponding power spectral density function have been derived based on the model; these functions are compared with the experimental results.

THEORETICAL

In a gas-solids fluidized bed, bubbles appear at any locale in the bed. The pressure fluctuations caused by bubble movements can be measured by means of a pressure probe (Lirag and Littman, 1971; Fan et al., 1981); the detailed bubbling phenomena can be characterized by the auto-correlation function and the power spectrum of the signals from the probe. Moreover, stochastic characteristics of the bubble behavior can be reasonably determined from analyzing these auto-correlation functions. The auto-correlation function is a manifestation of the change in the void fraction in the bed and contains two basic components; one essentially is a regular periodic or wave-like component generated by the passage of bubbles through the probe field, and the other the random component, due mainly to the stochastic nature of bubble motion into and out of the field. The random component distorts the wave-like component. The power spectrum yields information related to the local velocity distribution of bubbles and the major bubbling frequency.

Each recorded signal is assumed to comprise two components. The first is the periodic or sine wave component, Y(t), measured from its mean value. This can be expressed as (Yutani et al., 1983)

$$Y(t) = A \sin(2\pi f_o t + \theta) \qquad (1)$$

where

A = amplitude

f_o = frequency in cycles per unit time

θ = initial phase angle with respect to the time origin in radians

Since a bubble enters the field of a probe in a random manner, θ is a random variable; it is assumed that θ is uniformly distributed with a probability density function of $p(\theta)$ over $(0,2\pi)$.

The second component is represented by a stochastic process describing the random passage of bubbles through the field, for which we define

$$Z(t) = \begin{cases} 1, & \text{if a bubble is in the field} \\ 0, & \text{otherwise} \end{cases} \qquad (2)$$

Note that $Z(t)$ is a continuous-time Markov process with two possible states, 0 and 1. This process is completely defined under the following assumptions (Chatfield, 1984);

$$Pr[Z(t+\Delta t) = 1 \,|\, Z(t) = 0] = \alpha \Delta t + o(\Delta t) \qquad (3)$$

and

$$Pr[Z(t+\Delta t) = 0 \,|\, Z(t) = 1] = \beta \Delta t + o(\Delta t) \qquad (4)$$

where α is the intensity of transition of a bubble from the outside to the inside of the field, and β from the inside to the outside. The expression in the left-hand side of

Eqs. 3 and 4, namely, $Pr[E_1 | E_2]$, denotes the conditional probability of event E_1 given event E_2.

Let

$$p_1(t) = Pr[Z(t) = 1] \tag{5}$$

Then, it can be shown that (see APPENDIX)

$$p_1(t) = \frac{\alpha}{(\alpha+\beta)} + [p_1(0) - \frac{\alpha}{(\alpha+\beta)}]e^{-(\alpha+\beta)t} \tag{6}$$

From the characteristics of the probe employed in the present work, we see that the wave-like component, Y(t), and the stochastic component, Z(t), of the recorded signals, X(t), are independent of each other; however, they occur simultaneously. Thus, we can write

$$X(t) = Y(t)Z(t) \tag{7}$$

Auto-Correlation Function

The auto-correlation function of random data describes the general dependence of the datum at one moment on that at another moment (see, e.g., Bendat, and Piersol, 1971). Consider a sampled time-history record of X(t); an estimation for the auto-correlation between the values of X(t) at times t and $(t + \tau)$ is obtained by taking the product of the two values and averaging over the observation time, T. The resultant average product will approach the exact auto-correlation function of X(t) as T approaches infinity, i.e.,

$$R_{XX}(\tau) = \lim_{T\to\infty} \frac{1}{T} \int_0^T X(t)X(t+\tau)dt \qquad (8)$$

Based on the assumption that the "ergodic hypothesis" is valid for the system under consideration, the auto-correlation function is equal to the corresponding ensemble averaged value, i.e.,

$$R_{XX}(\tau) = E[X(t)X(t+\tau)]$$

$$= \int_{-\infty}^{\infty} \int_{-\infty}^{\infty} x_1 x_2 p(x_1, x_2; \tau) dx_1 dx_2 \qquad (9)$$

where $p(x_1, x_2; \tau)$ is the joint probability density function of $X(t)$ and $X(t+\tau)$.

Applying the definitions of the auto-correlation function, as given by Eq. 9, and periodic component of the recorded signals, $Y(t)$, given by Eq. 1, we have

$$R_{YY}(\tau) = \int_0^{2\pi} A \sin(2\pi f_o t+\theta)\ A \sin[2\pi f_o(t+\tau)+ \theta]p(\theta)d\theta$$

$$= \frac{A^2}{2} \cos(2\pi f_o \tau) \qquad (10)$$

Since $Z(t)$ is assumed to be a stationary random process, the auto-correlation of $Z(t)$ can be derived as (see APPENDIX)

$$R_{ZZ}(\tau) = \gamma e^{-\lambda\tau} \qquad (11)$$

Since $Y(t)$ and $Z(t)$ are independent of each other, Eq. 7 indicates that the auto-correlation function of $X(t)$ can be written as (see, e.g., Bendat and Piersol, 1971)

$$R_{xx}(\tau) = R_{yy}(\tau)R_{zz}(\tau) \tag{12}$$

Substitution of Eqs. 10 and 11 into Eq. 12 gives

$$R_{xx}(\tau) = \frac{\gamma A^2}{2} e^{-\lambda\tau} \cos(2\pi f_o \tau) \tag{13}$$

Normalizing the auto-correlation function, we have

$$R^*_{xx}(\tau) = \frac{R_{xx}(\tau)}{R_{xx}(0)} = e^{-\lambda\tau} \cos(2\pi f_o \tau) \tag{14}$$

Power Spectrum

The power spectral density function of X(t), $G_{xx}(\omega)$, is defined as (see, e.g., Bendat and Piersol, 1971)

$$G_{xx}(\omega) = \frac{2}{\pi} \int_0^\infty R_{xx}(\tau) \cos(\omega\tau) d\tau \tag{15}$$

Substituting Eq. 13 into this expression and integrating, we have

$$G_{xx}(\omega) = \frac{\gamma\lambda A^2}{\pi} \left[\frac{\omega^2+(\lambda^2+c^2)}{\omega^4 + 2(\lambda^2-c^2)\omega^2+(\lambda^2+c^2)^2}\right] \tag{16}$$

where

$$c = 2\pi f_o \tag{17}$$

At the stationary point in $G_{xx}(\omega)$, the condition

$$\dot{G}_{xx}(\omega) = \frac{\gamma\lambda A^2}{\pi} \frac{(-2\omega)[\omega^4+2(\lambda^2+c^2)\omega^2+(\lambda^4-2\lambda^2c^2-3c^4]}{[\omega^4+2(\lambda^2-c^2)\omega^2+(\lambda^2+c^2)^2]^2} = 0 \tag{18}$$

holds. The value of ω satisfying this condition is

$$\omega = (\lambda^2 + c^2)^{1/4} \; [2c-(\lambda^2+c^2)^{1/2}]^{1/2} = \omega_1 \qquad (19)$$

We find also that the value of the second derivative at this point is negative, i.e.,

$$\ddot{G}_{xx}(\omega)|_{\omega=\omega_1} < 0$$

Thus, a single maximum of $G_{xx}(\omega)$ occurs at ω_1, and the corresponding value of this maximum is

$$G_{xx}(\omega_1) = \frac{\gamma\lambda A^2}{4\pi c} \frac{1}{[(\lambda^2+c^2)^{1/2}-c]} \qquad (20)$$

EXPERIMENTAL

The facilities and procedure employed in carrying out experiments and measurements are described in this section.

Facilities

A schematic diagram of the experimental facilities is shown in Figure 1. The fluidized bed employed consisted of a bed proper, a distributor, and a plenum column. The bed proper and the plenum column were fabricated from "Plexiglass" to permit visual observation. Their diameter was 0.203m (8 in.), and their heights were 0.61m (24 in.) and 0.17m (6.7 in.),respectively. The distributor was perforated aluminum plates, 0.00158m (1/16 in.) thick and had 164 holes. The layout of holes in the distributor is shown in Figure 2. Sand served as the fluidized particles, and air at 30-35°C the fluidizing medium. The physical properties of the sand and the experimental conditions are summarized in Table 1.

A pressure tap was installed on the wall of the bed column immediately above the distributor. The inside opening of the tap was covered with a screen to prevent the sand from entering the tap. The outside opening of the tap was connected to one of the two input channels of a differential pressure transducer (Enterprise Model CJ3D), which produced an output voltage proportional to the pressure difference between two channels. The remaining

channel was exposed to the atmosphere, and thus, the fluctuations of pressure drop across the entire bed were measured. The working capacity of the transducer was ± 6.90 kPa (± 1 psi). Signal processing was accomplished with the aid of a Bascom-Turner digital recorder, an IBM PC, and a main frame (NAS 6630) computer.

Procedure

For each run of the experiment, the pressure fluctuations of the bed were detected by connecting the tap to the pressure transducer. The voltage-time signal (corresponding to the pressure-time signal) from the transducer was fed to the recorder at a selected sampling rate. The sampling rate was 20 ms. A typical sample consisted of 2000 points. This combination of sampling rate and sample length ensured the capturing of the full spectrum of hydrodynamic signal for the gas-solid fluidized bed (typically 25 Hz). A RS-232 interface was used to send the signals from recorder to the PC. The signals were then sent to the main frame computer via a 1200 baud modem for off-line time-series analysis.

CALCULATIONS

All analysis of data were carried out off-line in the main frame computer utilizing the 1982 version of the SAS (Statistical Analysis System) Package. The statistical properties of the pressure fluctuation signals calculated were the mean, variance, auto-correlation function and power spectral density function.

We resorted to non-linear regression analysis to fit the model in terms of the auto-correlation function, given by Eq. 14, to the experimental auto-correlation function by manipulating the frequency, f_o, and the intensity, λ. The normalized power spectral density function, $G_{xx}(w)/G_{xx}(w_1)$, was obtained by dividing Eq. 16 by Eq. 20. This was done to eliminate the parameter γ. This spectral density function ratio based on the model was plotted over the spectral density function, obtained from the experimental data, to examine goodness of the fit. The calculations were repeated for six different superficial velocities of the fluidizing gas.

RESULTS AND DISCUSSION

Typical signals recorded from the pressure transducer are traced in Figures 3 and 4, with superficial velocity of the fluidizing gas as the parameter. It appears that each tracing of the recorded signals at a given superficial velocity contains wave-like signals with various frequencies. In other words, each tracing of the recorded signals is composed of a random or stochastic component and a wave-like or sine component. The variance or the magnitude of each signal increases with the increase in the superficial velocity. The trend for the amplitude to increase with the air flow rate was expected since the bubble size became larger when air flow rate was increased. The corresponding auto-correlation functions of the recorded pressure-fluctuation signals at different superficial velocities are illustrated in Figure 5 through 10. The shape of the auto-correlation function is substantially influenced by the hydrodynamics of the bed which is directly related to the pattern of bubbling. Thus, analysis of the auto-correlation function of each signal gives rise to statistical information concerning the bubble behavior.

Comparison of the Model to Experimental Data

The auto-correlation function based on the model, Eq. 14, has been fitted to that obtained experimentally by

varying the frequency, f_o, and the intensity, λ, by means of a non-linear regression analysis. These are illustrated in Figures 5 through 10. The dashed lines in these figures represent the model equation. We see that the greater the superficial velocity, the faster the decay of the auto-correlation function. This implies that the intensity of bubble motion increases with the increase in the air flow rate, i.e., the random component of the recorded signals becomes pronounced compared to the wave-like signals. Figure 11 illustrates the relationship between the intensity of bubbling, λ, and the superficial velocity u; it confirms that λ increases with u.

The frequency corresponding to the first major peak of the auto-correlation function beyond the null delay (τ=0) is identified as the dominant frequency, f_o. The values of f_o at various superficial velocities obtained from the auto-correlation functions are given in Table 2; note that f_o decreases as u increases. This may be attributed to the fact that the size of the bubbles formed is bigger at a higher air flow rate.

Power Spectrum

The experimentally obtained pressure fluctuation signals have been analyzed and the corresponding power spectral density functions are plotted as solid lines in

Figures 12 through 17 at different superficial velocities of the fluidizing medium. The most obvious and yet most important feature of the power spectral density obtained in all runs is the presence of a sharp peak. The location and other characteristics of the peaks depend on the bed parameters. The concentration of the power of the signal into a very narrow frequency band of less than 1 Hz confirms the presence of a periodic component in the pressure signals (see, e.g., Bendat and Piersol, 1971). Essentially, the same frequency is always obtained from the power spectrum and the auto-correlation functions as shown in Table 2 for various superficial gas velocities; obviously, the auto-correlation and power spectral density functions are all consistent with one another. This clearly demonstrates the presence of a periodic component in the pressure fluctuation signals.

The power spectrum provides more detailed information than the auto-correlation function on the bubble movement. We observe in Figures 12 through 17 that as u increases, additional small peaks appear in the spectral density plots, thereby indicating a definite trend in the power spectrum, which shifts from a predominately wave-like pattern to a predominant random pattern. This is consistent with the observations made from the auto correlation function plots that as u increases, λ

(intensity of bubbling) also increases, i.e. the random component becomes predominant.

The power spectral density function based on the model, $G_{xx}(\omega)$, is obtained from the auto-correlation function $R_{xx}(\tau)$ according to Eq. 15. In Figures 12 through 17, the experimentally determined functions are compared with those calculated from the model in Figure 12 through 17. Notice that the value of the peak frequency ($= \omega_1/2\pi$) of the power spectral density function calculated from the model is in good agreement with that of the frequency, f_o, determined from the experimental data (see also Table 2).

Relationship between the Frequency and Superficial Velocity

As delineated in the introductory section, there seems to be both theoretical and experimental variation in the results of the various investigators regarding the effect of the superficial velocity of the fluidizing medium on the frequency of pressure fluctuations. Hiby (1967) has proposed the following approximate relationships between the bed oscillation frequency, ν, and u for the two limiting cases of laminar flow and turbulent flow:

$$\nu \propto u^{-0.31} \text{ for the laminar flow} \qquad (21)$$

and

$$\nu \propto u^{-1} \text{ for the turbulent flow} \qquad (22)$$

According to Hiby, the higher the amplitude of oscillation, as a result of higher porosity, the smaller the number of layers which can sustain joint oscillations. Nevertheless, his experimental results are not in confirmity with these relations. He has attributed this to the fact that $h/\bar{d}_p$ in his experiment was equal to only 10; a smaller effective height could have meant an increase in the average natural frequency of the coherent part of the bed, which in the process would counteract the decrease expected from Eqs. 21 and 22.

In the present work the probe was located about 2 cm from the distributor; this makes $h/\bar{d}_p$ approximately 200, if h is considered to be the probe distance from the distributor. In Hiby's experiments, the capacitive probe was located at the surface of the bed, thus making the probe distance from the distributor equal to the static bed height.

Based on Hiby's theory, an effort has been made in the present work to find an empirical relationship between u and the experimentally determined f_o. Figure 18 plots the inf_o vs inu. Note that the plot obeys the following relationship;

$$f_o \propto u^{-0.623} \qquad (23)$$

This approximate proportionality appears to fall within the range of the relationships proposed by Hiby for the laminar and turbulent flows (Eqs. 21 and 22).

Fan et al. (1981) have proposed that the formation of large bubbles through bubble coalescence in the main body or middle portion of the bed, the formation of small bubbles near the distributor and the jet flow immediately above the distributor affect the pressure fluctuations in the lower portion of a deep fluidized bed. The major fluctuations are caused by the formation of large bubbles and are transmitted downward from the middle portion of the bed. The small fluctuations, caused by the jet flow and the formation of small bubbles, are transmitted upward and are superimposed on the major fluctuations. The bed used in the present work was relatively shallow ($H_s/D = 0.542$); thus, bubble coalescence might have occurred immediately above the distributor, forming larger bubbles close to the probe. This could have impelled f_o to decrease with the increase in u. The intensity of bubbling, λ, increased with u, since the enhanced rate of air flow increased the rate of bubble formation near the distributor, thus increasing the randomness in the bed.

CONCLUSIONS

Pressure fluctuation signals from a gas-solids fluidized bed have been recorded and analyzed statistically. The auto-correlation and power spectral density functions of the pressure fluctuations are all consistent with one another; this clearly demonstrate the presence of a periodic component in the fluctuations. The amplitude of the recorded signals increased with an increase in the superficial velocity of the fluidizing medium, u and it has been found to affect the pressure fluctuations significantly. The frequency, f_o, decreased and the intensity of bubble motion, λ, increased when the superficial velocity was increased. This phenomena has been qualitatively interpreted.

The results of the experiment indicate that the recorded signals are composed of a wave-like component and a stochastic component. A stochastic model has been proposed by taking these two components into account. The auto-correlation and power spectral density functions of the resultant model have been fitted to those obtained experimentally by adjusting the model parameters, the dominant frequency, f_o, and the intensity of transition of bubbles, λ. The auto-correlation and power spectral density functions of the model are in good agreement with those obtained experimentally.

APPENDIX. Derivation of Eqs. 6 and 11

Let us consider a time-continuous Markov process Z(t) having two possible states, 0 and 1. According to the assumptions expressed in Eqs. 3 and 4 in the text, we can write the probability balance for $p_1(t)$ (defined in Eq. 5) as

$$p_1(t+\Delta t) = p_1(t)[1-\beta\Delta t] + [1-p_1(t)]\alpha\Delta t + o(\Delta t) \quad \text{(A-1)}$$

or

$$\frac{p_1(t+\Delta t) - p_1(t)}{\Delta t} = -(\alpha+\beta)p_1(t) + \alpha + \frac{o(\Delta t)}{\Delta t} \quad \text{(A-2)}$$

Taking the limit as $\Delta t \to 0$, we obtain

$$\frac{d}{dt} p_1(t) + (\alpha+\beta)p_1(t) = \alpha \quad \text{(A-3)}$$

Solving this expression yields

$$p_1(t) = \frac{\alpha}{\alpha+\beta} + \left[p_1(0) - \frac{\alpha}{\alpha+\beta}\right] e^{-(\alpha+\beta)t} \quad \text{(A-4)}$$

which is Eq. 6 in the text. If

$$p_1(0) = \frac{\alpha}{\alpha+\beta} ,$$

the process is said to be second order stationary (see, e.g. Chatfield, 1984).

The auto-correlation function of Z(t) is defined as

$$R_{zz}(t) = E[Z(t)Z(t+\tau)] \quad \text{(A-5)}$$

We can see immediately that the product of Z(t) and Z(t+τ) must take on only the values, 0 and 1. It will be equal to 1 if a bubble is in the field at both times t and (t+τ);

otherwise, it will be zero. Therefore, the expectation of the product to be equal to the probability of this event is

$$E[Z(t)Z(t+\tau)] = Pr[\text{both } Z(t) \text{ and } Z(t+\tau) \text{ are } 1]$$

$$= Pr[Z(t) = 1]Pr[Z(t+\tau) = 1 \,|\, Z(t) = 1] \quad \text{(A-6)}$$

If we assume Z(t) to be a time stationary process, we have

$$Pr[Z(t+\tau) = 1 \,|\, Z(t) = 1] = Pr[Z(\tau) = 1 \,|\, Z(0) = 1] \quad \text{(A-7)}$$

Thus, Eq. A-6 becomes

$$E[Z(t)Z(t+\tau)] = Pr[Z(t) = 1]Pr[Z(\tau) = 1 \,\big|\, Z(0) = 1]$$

$$= p_1(t)p_{11}(\tau) \quad \text{(A-8)}$$

Now considering the process to be second order stationary Eq. A-4 reduces to

$$p_1(t) = \frac{\alpha}{\alpha+\beta} \quad \text{(A-9)}$$

Substituting this expression into Eq. A-8 yields

$$E[Z(t)Z(t+\tau)] = \frac{\alpha}{\alpha+\beta}\, p_{11}(\tau) \quad \text{(A-10)}$$

The next step will be to calculate the transition probability $p_{11}(t)$. We utilize the Kolmogorov backward differential equations for a two-state Markov process with transition probabilities α and β, defined by Eqs. 3 and 4 in the text, respectively. This gives rise to the following set of differential equations;

$$\frac{d}{dt}\, p_{01}(t) = \alpha[p_{11}(t) - p_{01}(t)] \quad \text{(A-11)}$$

and

$$\frac{d}{dt} p_{11}(t) = \beta[p_{01}(t) - p_{11}(t)] \qquad \text{(A-12)}$$

Multiplying Eq. A-11 by β and Eq. A-12 by α and adding the resultant equations yield

$$\beta\dot{p}_{01}(t) + \alpha\dot{p}_{11}(t) = 0 \qquad \text{(A-13)}$$

By integrating and using the initial conditions

$$p_{01}(0) = 0 \text{ and } p_{11}(0) = 1, \qquad \text{(A-14)}$$

we obtain

$$\beta p_{01}(t) = \alpha[1-p_{11}(t)] \qquad \text{(A-15)}$$

Substituting Eq. A-15 into Eq. A-12 leads to

$$\dot{p}_{11}(t) = (\alpha+\beta)\left[\frac{\alpha}{\alpha+\beta} - p_{11}(t)\right] \qquad \text{(A-16)}$$

By solving this expression, subject to the initial condition $p_{11}(0) = 1$, we have

$$p_{11}(t) = \frac{\alpha}{\alpha+\beta} + \frac{\beta}{\alpha+\beta} e^{-(\alpha+\beta)t} \qquad \text{(A-17)}$$

and, therefore,

$$p_{11}(\tau) = \frac{\alpha}{\alpha+\beta} + \frac{\beta}{\alpha+\beta} e^{-(\alpha+\beta)\tau} \qquad \text{(A-18)}$$

Substituting this expression in Eq. A-10 gives

$$E[Z(t)Z(t+\tau)] = \frac{\alpha}{\alpha+\beta}\left[\frac{\alpha}{\alpha+\beta} + \frac{\beta}{\alpha+\beta} e^{-(\alpha+\beta)\tau}\right] \qquad \text{(A-19)}$$

or

$$R_{zz}(\tau) = \frac{\alpha^2}{(\alpha+\beta)^2} + \frac{\alpha\beta}{(\alpha+\beta)^2} e^{-(\alpha+\beta)\tau} \qquad \text{(A-20)}$$

For the steady-state operation, the probability that a bubble will enter the field is identical to that for the

reverse. Since the volume of the field compared with the total volume of the fluidized bed is very small, the intensity of exit from the field, β, is much larger than the intensity of transition from the outside to the inside of the field, α. For a sufficiently small value of τ, the first term on the right-hand side in Eq. A-20 is negligible. Consequently, Eq. A-20 may be rewritten as

$$R_{zz}(\tau) \approx \frac{\alpha\beta}{(\alpha+\beta)^2} e^{-(\alpha+\beta)\tau} = \gamma e^{-\lambda\tau} \qquad \text{(A-21)}$$

where

$$\lambda = (\alpha+\beta)$$

and

$$\gamma = \frac{\alpha\beta}{(\alpha+\beta)^2}$$

This is Eq. 11 in the text.

NOMENCLATURE

A	= amplitude of the sine wave component
c	= constant = $2\pi f_o$
$\bar{d}_p$	= average particle diameter, m
D	= diameter of the bed, m
f_o	= cyclic frequency of the sine wave component, Hz or 1/s
$G_{xx}(\omega)$	= power spectral density function of X(t)
$G_{xx}(\omega_1)$	= maximum value of $G_{xx}(\omega)$
H_s	= static bed height, m
H_{mv}	= bed height at minimum fluidization, m
h	= height of the probe from the distributor, m
$Pr[E_1 \mid E_2]$	= conditional probability of event E_1 given event E_2
$p(\theta)$	= probability density function of θ
$p_1(t)$	= Pr[Z(t)=1], absolute probability
$p_{ij}(t)$	= Pr[Z(t)=j|Z(0)=i], transition probability
$p(x_1,x_2;\tau)$	= joint probability density function of X(t) and X(t+τ)
$R_{xx}(\tau)$	= auto-correlation function of X(t)
$R^*_{xx}(\tau)$	= normalized auto-correlation function of X(ϵ)
$R_{yy}(\tau)$	= auto-correlation function of Y(t)
$R_{zz}(\tau)$	= auto-correlation function of Z(t)

T = duration of the sample signal, s

t = time, s

u = superficial velocity of the fluidizing medium, m/s

u_{mf} = minimum fluidizing velocity, m/s

$X(t)$ = signal recorded from the pressure probe

$Y(t)$ = sine wave component or wave-like signal

$Z(t)$ = stochastic or random component

Greek Letters

α = intensity of transition of a bubble from the outside of the field to the inside

β = intensity of transition of a bubble from the inside of the field to the outside

ϵ_{mf} = voidage at minimum fluidization

γ = constant = $\alpha\beta/(\alpha+\beta)^2$

ν = oscillation frequency of the bed (from Hiby's, 1967, paper), Hz or 1/s

θ = initial phase angle with respect to the time origin, radians

τ = time shift variable, s

λ = constant = $(\alpha+\beta)$, 1/s

ω = angular frequency, radian/s

ω_1 = stationary point of $G_{xx}(\omega)$, radian/sec

LITERATURE CITED

Bendat, J. S. and A. G. Piersol, *Random Data: Analysis and Measurement Procedures*, Chapters 1,3, and 7, Wiley-Interscience, New York (1971).

Chatfield, C., *The Analysis of Time Series: An Introduction*, Chapters 1,2, and 3, Chapman and Hall, New York (1984).

Fan, L. T., T. C. Ho, S. Hiraoka, and W. P. Walawender, "Pressure Fluctuations in a Fluidized Bed," AIChE Journal, 27, 388-396 (1981).

Hiby, J. W., "Periodic Phenomena Connected with Gas-Solid Fluidization," Proceedings of the International Symposium on Fluidization, Eindhoven, pp. 99-112, Netherlands University Press, Amsterdam, Holland (1967).

Jones, B. R. E. and D. L. Pyle, "On Stability, Dynamics, and Bubbling in Fluidized Beds," AIChE Symposium Series, No. 116, 67, 1-10 (1971).

Kang, W. K., J. P. Sutherland, and G. L. Osberg, "Pressure Fluctuations in a Fluidized Bed with and without Screen Cylindrical Packings," Ind. Eng. Chem. Fundamentals, 6, 499-504 (1967).

Lirag, R. C. and H. Littman, "Statistical Study of the Pressure Fluctuations in a Fluidized Bed," AIChE Symposium Series, No. 116, 67, 11-22 (1971).

Moritomi, H., S. Mori, K. Araki, and A. Moriyama, "Periodic Pressure Fluctuations in a Gaseous Fluidized Bed," Kagaku Kogaku Ronbunshu, 6, 392-396(1980).

Shuster, W. and P. Kisliak, "The Measurement of Fluidization Quality," Chem. Eng. Progr., 48, 455-458 (1952).

Sutherland, K. S., "The Effect of Particle Size on the Properties of Gas-Fluidized Beds," AEC Research and Development Report, ANL-6907, Argonne National Lab., Argonne, Illinois (1964).

Tamarin, A. I., "The Origin of Self-Excited Oscillations in Fluidized Beds," International Chem. Eng., 4, 50-54 (1964).

Whitehead, A. B., D. C. Dent, and C. H. McAdam, "Fluidization Studies in Large Gas-Solid Systems. Part V: Long and Short Term Pressure Instabilities," Powder Technology, 18, 231-237 (1977).

Winter, O., "Density and Pressure Fluctuations in Gas Fluidized Beds," AIChE, 14, 427-434 (1968).

Wong, H. W. and M. H. I. Baird, "Fluidization in a Pulsed Gas Flow," The Chem. Eng. Journal, 2, 104-7 (1971).

Yutani, N., L. T. Fan, and J. R. Too, "Behavior of Particles in a Liquid-Solids Fluidized Bed," AIChE J., 29, 101-106 (1983).

Table 1. Physical Properties of Sand and Test Ranges of Experimental Variables.

Experimental Variables	Test Range
Sand Size	Sieve No. - 30~↑40
Density of Sand	2620 kg/m^3
$\bar{d}p$	0.000491m
u_{mf}	0.25 m/s
u	0.54 - 0.98 m/s
ϵ_{mf}	0.47
H_s	0.08-0.09 m
H_{mf}	0.11-0.12 m

Table 2. Effect of Superficial Velocity u on Major Frequency and Intensity of Bubbling.

u, m/s	λ from Eq. 14	Major Frequency, Hz: f_o from the auto-correlation function (experimental)	f_o from the spectral density function (experimental)	$\omega_{1/2\pi}$ from Eq. 19.
0.54318	1.965	5.75	5.700	5.75701
0.60836	3.480	5.40	5.275	5.37601
0.65182	3.585	5.10	4.925	5.09553
0.76040	4.335	4.60	4.325	4.58592
0.86908	3.600	4.15	4.050	4.09439
0.97770	4.500	4.12	3.975	4.11737

1 Rotameter
2 Pressure gauge
3 Temperature gauge
4 Plenum
5 Distributor
6 Bed
7 Screen
8 Pressure tap
9 Pressure transducer
10 Strip chart recorder
11 Bascom turner Recorder
12 SAS package
13 MAIN FRAME
14 IBM PC
15 Modem
16 Drying tube
17 Manometer (used for calibration)
18-26 valves

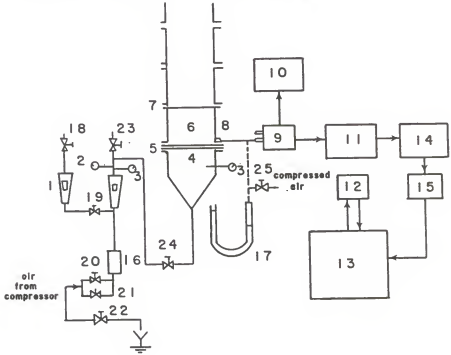

Figure 1. Experimental setup.

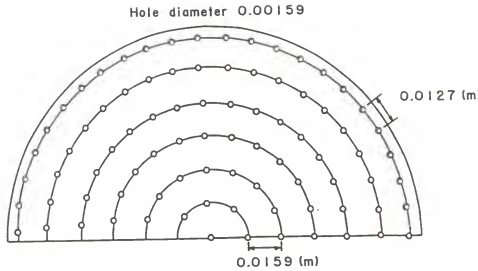

Figure 2. Hole layout of the distributer.

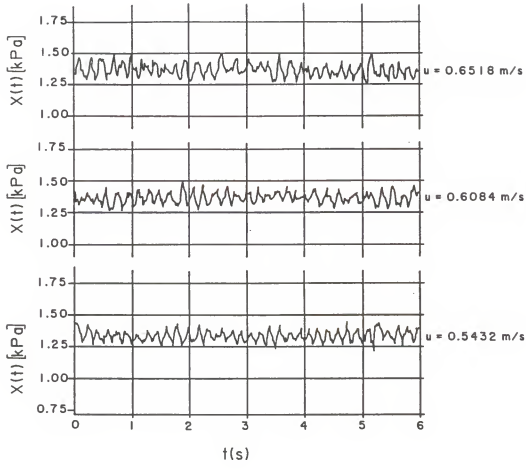

Figure 3. Pressure fluctuation signal at various superficial velocity of the fluidizing medium.

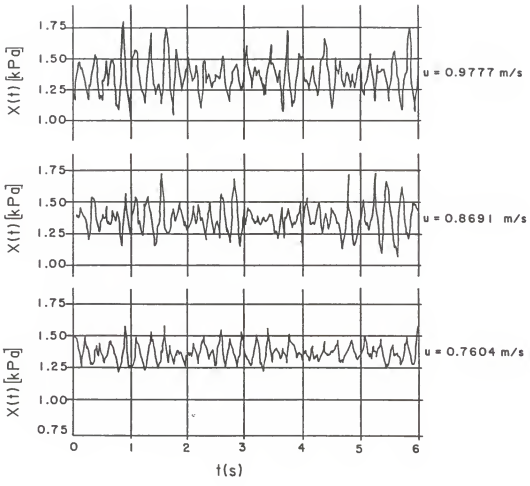

Figure 4. Pressure fluctuation signal at various superficial velocity of the fluidizing medium.

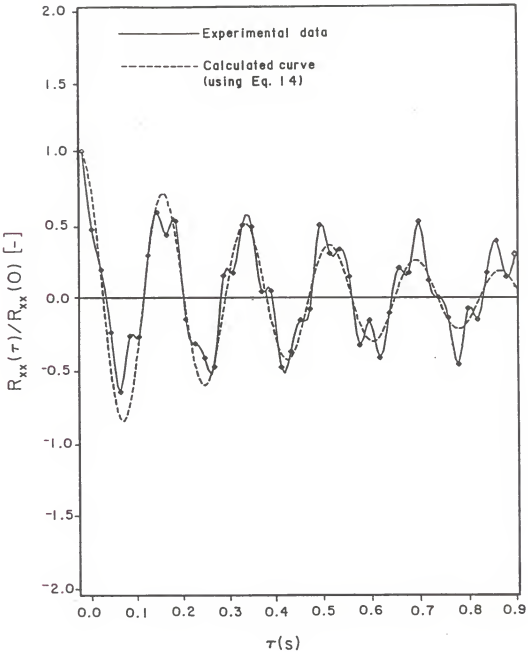

Figure 5. Comparison of the auto-correlation functions based on the model with that obtained from the experimental data at u = 0.5432 m/s.

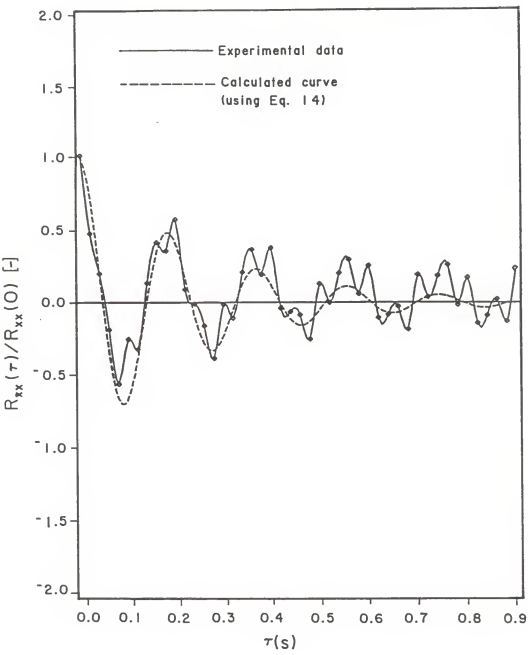

Figure 6. Comparison of the auto-correlation function based on the model with that obtained from the experimental data at u = 0.6084 m/s.

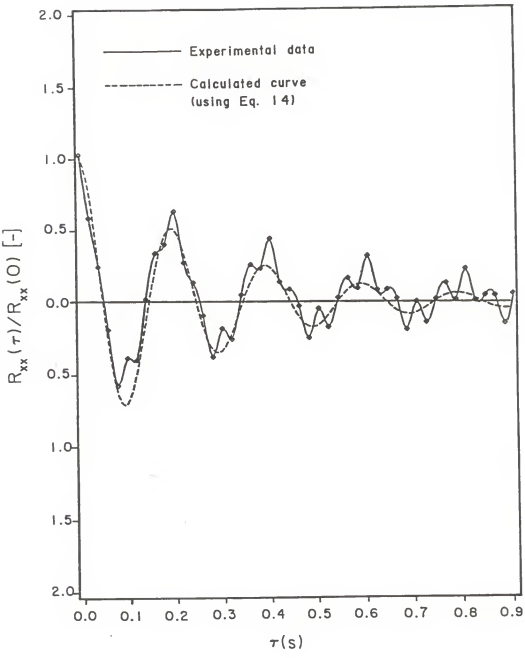

Figure 7. Comparison of the auto-correlation function based on the model with that obtained from the experimental data at u = 0.65182 m/s.

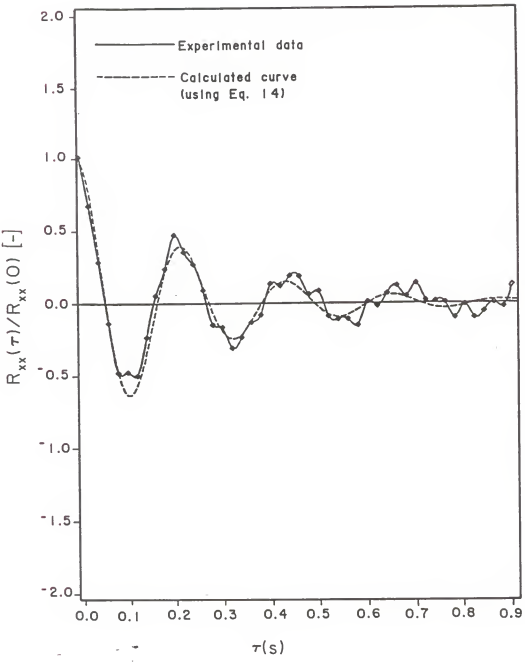

Figure 8. Comparison of the auto-correlation function based on the model with that obtained from the experimental data at u = 0.7604 m/s.

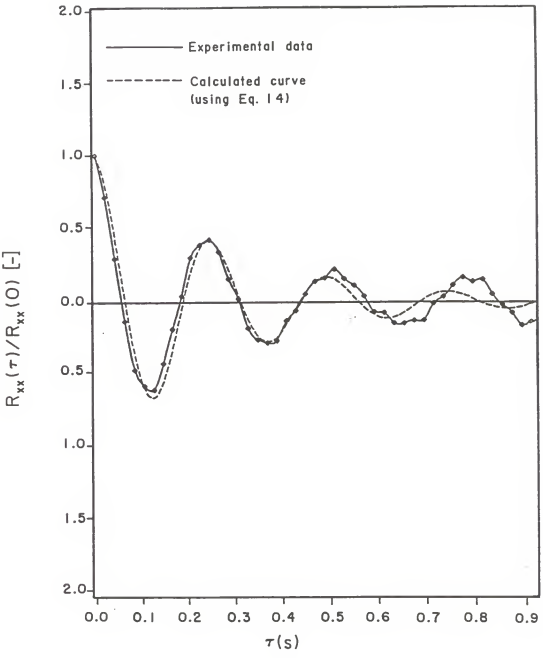

Figure 9. Comparison of the auto-correlation function based on the model with that obtained from the experimental data at u = 0.8691 m/s.

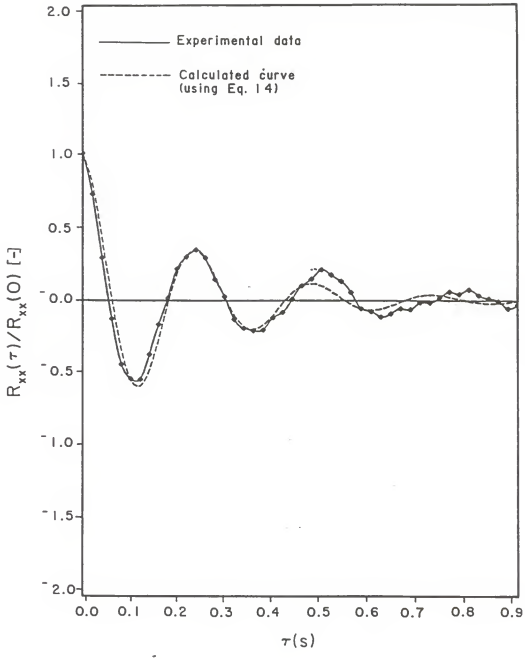

Figure 10. Comparison of the auto-correlation function based on the model with that obtained from the experimental data at u = 0.9777 m/s.

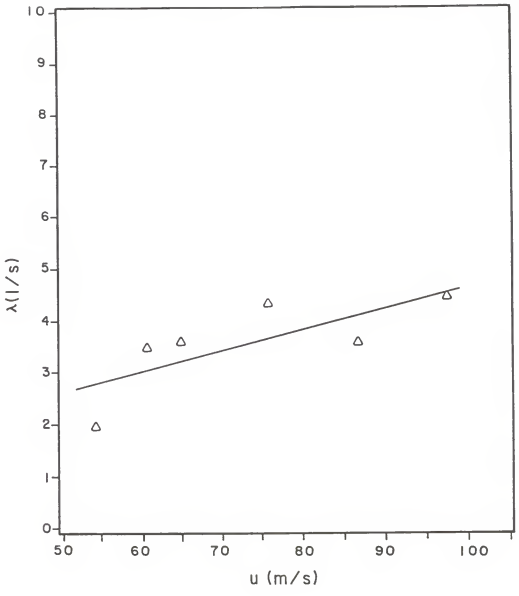

Figure 11. Plot of λ , intensity of bubbling vs u, superficial velocity.

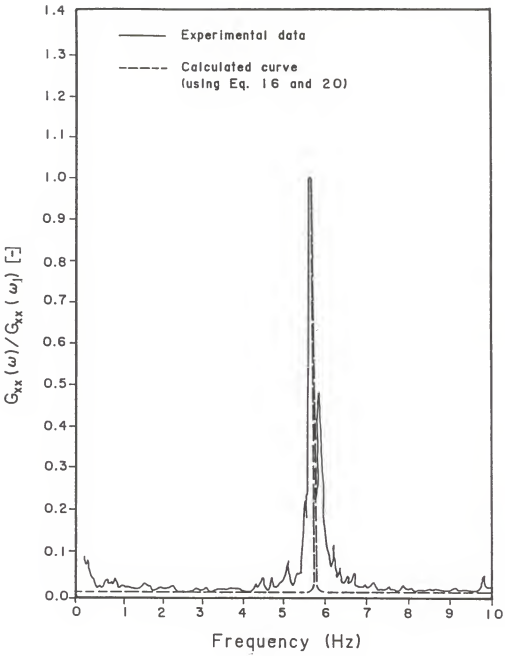

Figure 12. Comparison of the power spectral density funtion based on the model with that obtained from the experimental data at u = 0.5432 m/s.

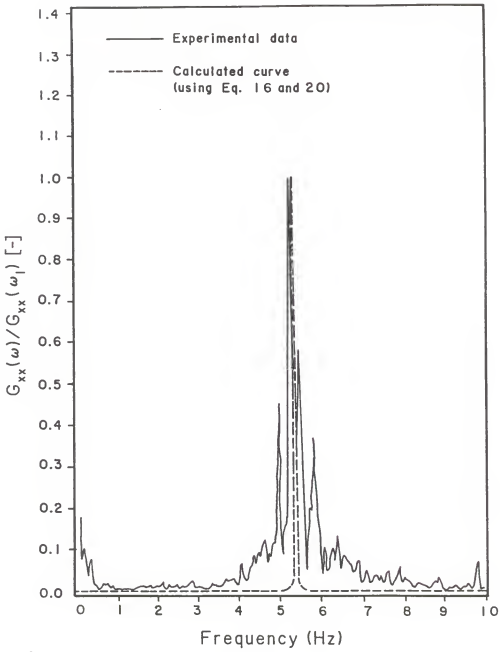

Figure 13. Comparison of the power spectral density funtion based on the model with that obtained from the experimental data at u = 0.6084 m/s.

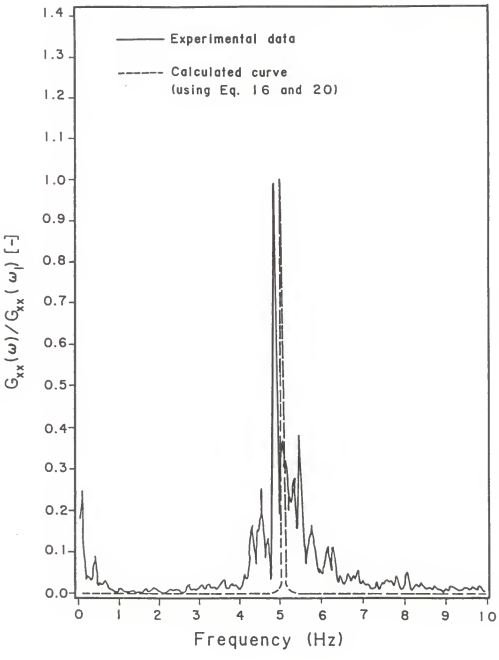

Figure 14. Comparison of the power spectral density funtion based on the model with that obtained from the experimental data at u = 0.6518 m/s.

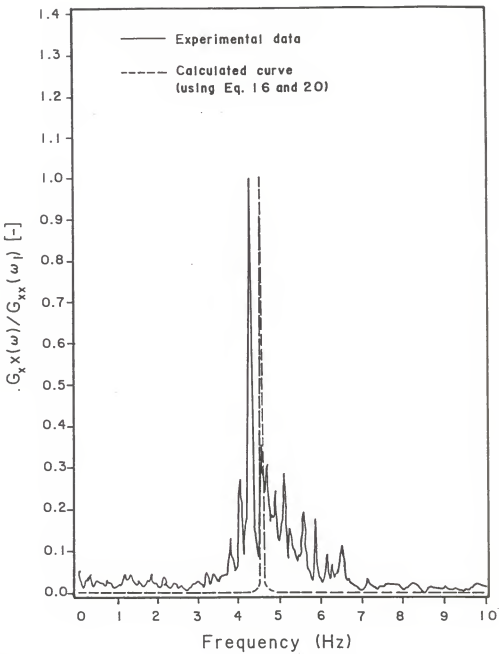

Figure 15. Comparison of the power spectral density funtion based on the model with that obtained from the experimental data at u = 0.7604 m/s.

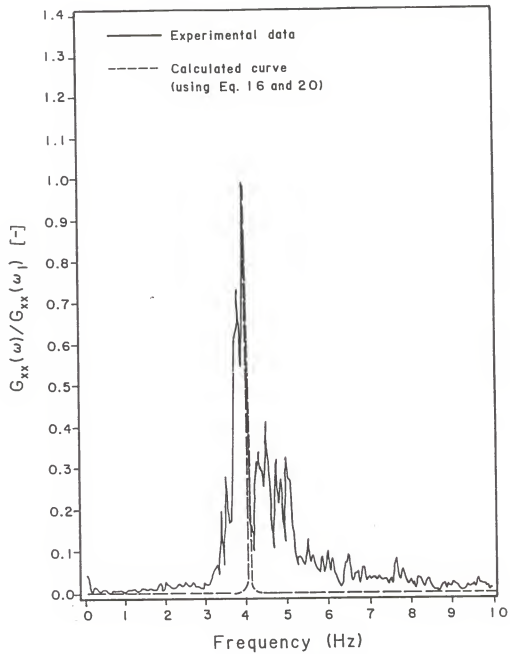

Figure 16. Comparison of the power spectral density funtion based on the model with that obtained from the experimental data at u = 0.8691 m/s.

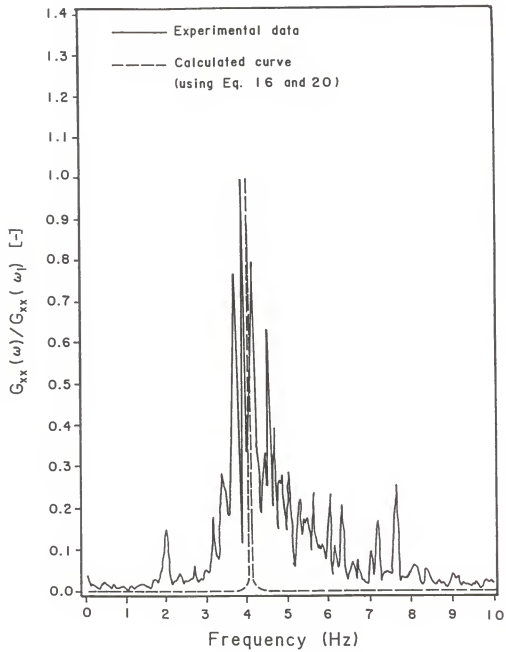

Figure 17. Comparison of the power spectral density funtion based on the model with that obtained from the experimental data at u = 0.9777 m/s.

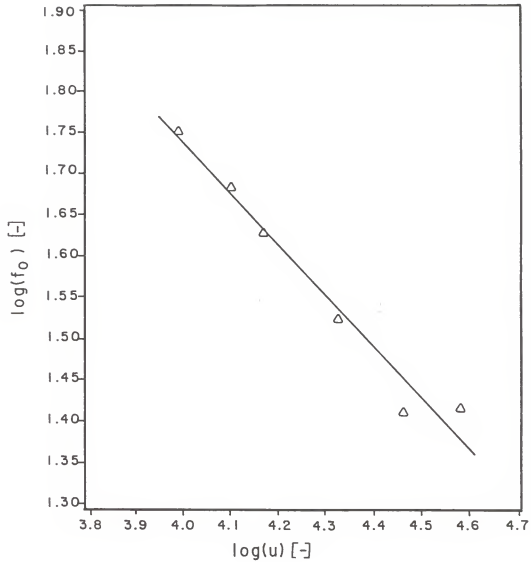

Figure 18. Plot of $\log(f_o)$ vs $\log(u)$.

A STOCHASTIC ANALYSIS OF PRESSURE FLUCTUATION IN A FLUIDIZED BED REACTOR

by

DEBASHIS NEOGI

B.Tech. (Chem. Engg.), Indian Institute of Technology, 1981
M.S. (Chem. Engg.), Kansas State University, 1984

AN ABSTRACT OF A MASTER'S REPORT

submitted in partial fulfillment of the

requirements for the degree

MASTER OF SCIENCE

Department of Statistics

KANSAS STATE UNIVERSITY
Manhattan, Kansas

1987

ABSTRACT

The characteristics of a gas-solid fluidized bed are influenced by complicated and stochastic phenomena, e.g., jetting and bubbling of the fluidizing medium and the motion of the fluidized particles. In this study pressure fluctuations due to the bubble movement were measured by means of a pressure probe over a range of time. The resultant time-series have been analyzed by determining their auto-correlation function and power spectrum with emphasis on the examination of the effect of the superficial velocity of the fluidizing gas. A stochastic model of bubble motion in a fluidized bed has been developed. This model visualizes the bubble motion in a fluidized bed to consist of the random movement, generating irregular signals, and the linear movement, generating wave-like signals. A theoretical auto-correlation function and a power spectral density function have been derived based on the model.